Diabetologia (2018) 61:1411–1423
https://doi.org/10.1007/s00125-018-4602-6

ARTICLE

Altered mitochondrial bioenergetics and ultrastructure in the skeletal muscle of young adults with type 1 diabetes

Cynthia M. F. Monaco[1] · Meghan C. Hughes[2] · Sofhia V. Ramos[2] · Nina E. Varah[1] · Christian Lamberz[3] · Fasih A. Rahman[4] · Chris McGlory[5] · Mark A. Tarnopolsky[6] · Matthew P. Krause[4] · Robert Laham[2] · Thomas J. Hawke[1] · Christopher G. R. Perry[2]

Received: 8 November 2017 / Accepted: 28 February 2018 / Published online: 18 April 2018

Abstract

Aims/hypothesis A comprehensive assessment of skeletal muscle ultrastructure and mitochondrial bioenergetics has not been undertaken in individuals with type 1 diabetes. This study aimed to systematically assess skeletal muscle mitochondrial phenotype in young adults with type 1 diabetes.

Methods Physically active, young adults (men and women) with type 1 diabetes (HbA_{1c} 63.0 ± 16.0 mmol/mol [7.9% ± 1.5%]) and without type 1 diabetes (control), matched for sex, age, BMI and level of physical activity, were recruited (n = 12/group) to undergo vastus lateralis muscle microbiopsies. Mitochondrial respiration (high-resolution respirometry), site-specific mitochondrial H_2O_2 emission and Ca^{2+} retention capacity (CRC) (spectrofluorometry) were assessed using permeabilised myofibre bundles. Electron microscopy and tomography were used to quantify mitochondrial content and investigate muscle ultrastructure. Skeletal muscle microvasculature was assessed by immunofluorescence.

Results Mitochondrial oxidative capacity was significantly lower in participants with type 1 diabetes vs the control group, specifically at Complex II of the electron transport chain, without differences in mitochondrial content between groups. Muscles of those with type 1 diabetes also exhibited increased mitochondrial H_2O_2 emission at Complex III and decreased CRC relative to control individuals. Electron tomography revealed an increase in the size and number of autophagic remnants in the muscles of participants with type 1 diabetes. Despite this, levels of the autophagic regulatory protein, phosphorylated AMP-activated protein kinase (p-AMPKα^{Thr172}), and its downstream targets, phosphorylated Unc-51 like autophagy activating kinase 1 (p-ULK1^{Ser555}) and p62, was similar between groups. In addition, no differences in muscle capillary density or platelet aggregation were observed between the groups.

Conclusions/interpretation Alterations in mitochondrial ultrastructure and bioenergetics are evident within the skeletal muscle of active young adults with type 1 diabetes. It is yet to be elucidated whether more rigorous exercise may help to prevent skeletal muscle metabolic deficiencies in both active and inactive individuals with type 1 diabetes.

Cynthia M. F. Monaco and Meghan C. Hughes are joint first authors. Thomas J. Hawke and Christopher G. R. Perry are joint senior authors.

Electronic supplementary material The online version of this article (https://doi.org/10.1007/s00125-018-4602-6) contains peer-reviewed but unedited supplementary material, which is available to authorised users.

✉ Thomas J. Hawke
hawke@mcmaster.ca

[1] Department of Pathology and Molecular Medicine, McMaster University, 4N65 Health Sciences Centre, 1200 Main Street West, Hamilton, ON L8N 3Z5, Canada

[2] School of Kinesiology and Health Sciences, Muscle Health Research Centre, York University, Toronto, ON, Canada

[3] German Center for Neurodegenerative Diseases (DZNE), Bonn, Germany

[4] Department of Kinesiology, University of Windsor, Windsor, ON, Canada

[5] Department of Kinesiology, McMaster University, Hamilton, ON, Canada

[6] Department of Pediatrics, McMaster University, Hamilton, ON, Canada

Research in context

What is already known about this subject?

- Previous research using ^{31}P-magnetic resonance spectroscopy (MRS) has reported a reduction in ATP synthesis rates in the skeletal muscle of those with type 1 diabetes; a finding that suggests mitochondrial impairment
- Skeletal muscle, by virtue of its mass, is the largest site for postprandial glucose disposal and is indispensable for glycaemic control
- Skeletal muscle mitochondrial impairments have been implicated in a number of pathophysiological states, including insulin resistance, type 2 diabetes, ageing and cachexia

What is the key question?

- Do skeletal muscle metabolic and ultrastructural abnormalities exist in physically active young adults with moderately controlled type 1 diabetes?

What are the new findings?

- Type 1 diabetes causes site-specific alterations in mitochondrial bioenergetics, including increases in H_2O_2 emission and decreases in mitochondrial respiration, as well as decreased mitochondrial Ca^{2+} retention capacity (CRC)
- Increases in autophagic debris were noted in the skeletal muscle of those with type 1 diabetes, without increases in the autophagic regulatory protein phosphorylated AMP-activated protein kinase (p-AMPKα^{Thr172}) and downstream autophagic proteins phosphorylated Unc-51 like autophagy activating kinase 1 (p-ULK1^{Ser555}) and p62
- Individuals with type 1 diabetes did not have reduced mitochondrial content or skeletal muscle capillary density, suggesting differences in mitochondrial bioenergetics and CRC are the result of intrinsic alterations

How might this impact on clinical practice in the foreseeable future?

- These findings indicate that recreational physical activity may be insufficient to prevent skeletal muscle metabolic deficiencies in type 1 diabetes. Further studies are required to elucidate whether more rigorous exercise may help to prevent skeletal muscle metabolic and ultrastructural abnormalities

Keywords Calcium tolerance · Capillary density · Mitochondria · Myopathy · Reactive oxygen species · Skeletal muscle · Type 1 diabetes

Abbreviations

AMPK	AMP-activated protein kinase
CRC	Ca^{2+} retention capacity
mG3PDH	Mitochondrial glycerol-3-phosphate dehydrogenase
mPTP	Mitochondrial permeability transition pore
MRS	Magnetic resonance spectroscopy
OXPHOS	Oxidative phosphorylation cocktail
PDC	Pyruvate dehydrogenase complex
ROS	Reactive oxygen species
TEM	Transmission electron microscopy
ULK1	Unc-51 like autophagy activating kinase 1

Introduction

Skeletal muscle accounts for almost half of our body weight and, as such, is responsible for up to 75% of insulin-stimulated glucose disposal after a meal [1, 2]. In fact, blood glucose uptake into muscle and its subsequent conversion to glycogen is a major determinant of insulin sensitivity [3, 4]. Given the importance of skeletal muscle for glucose management, as well as its vital role in insulin action, impairments in skeletal muscle health in people with type 1 diabetes diminishes their ability to mitigate dysglycaemic burdens, promotes the development and progression of complications [5, 6] and, ultimately, expedites the accelerated physical disability that characterises diabetes [7]. However, our understanding of the impact of this chronic disease on the health/quality of human skeletal muscle is extremely limited.

Mitochondria play a fundamental role in energy metabolism and ATP production throughout the body. Based on their role in fuel oxidation, mitochondria can also generate considerable amounts of reactive oxygen species (ROS). It remains controversial whether impaired skeletal muscle mitochondrial respiratory function contributes to insulin resistance and dysglycaemia in obesity and type 2 diabetes [8]. However, a consistent observation has been increased mitochondrial ROS in obese/type 2 diabetes relative to lean control individuals

[8]. In addition, using ^{31}P-magnetic resonance spectroscopy (MRS), people with type 1 diabetes have been shown to exhibit slowed post-exercise ATP resynthesis [9–11]; the underlying mechanism(s) for this impairment is currently unknown and would require a direct and comprehensive exploration of site-specific mitochondrial respiratory function. Moreover, the effect of type 1 diabetes on skeletal muscle ultrastructure, last reported in 1977 [12], has not been re-examined since the introduction of more aggressive insulin therapies (e.g. basal and fast-acting insulins, insulin analogues and pump therapy), and its effect on muscle mitochondrial ROS production remains to be elucidated.

Here, we hypothesised that otherwise healthy, young adults with type 1 diabetes would display site-specific decrements in skeletal muscle mitochondrial respiration, increased ROS production and altered muscle ultrastructure relative to non-diabetic controls.

Methods

Participants

Twelve untrained participants with type 1 diabetes were recruited and closely matched with twelve participants without diabetes (control group) for age, sex, BMI and level of physical activity. Demographics (Table 1) and participant number was determined by power calculations from our previous studies in human muscle [13, 14]. All participants with type 1 diabetes used insulin (insulin pump or multiple daily injections) and reported no complications. Prior to giving informed consent, all participants were given oral and written information about the experimental procedures. All procedures were approved by the Research Ethics Board at York University (REB number e2013-032) and conformed to the Declaration of Helsinki.

Study design

Participants reported to York University in the early morning or early afternoon and were instructed to consume a standardised meal 1.5–2 h prior to their visit. Participants with type 1 diabetes were also instructed to continue their habitual use of insulin. Upon arrival, body mass and height measurements were taken to determine BMI, and a blood sample was obtained using venepuncture, for HbA_{1c} analysis. Skeletal muscle samples were then obtained from the vastus lateralis muscle by a microbiopsy percutaneous needle, as described previously [13], and used for mitochondrial bioenergetic analyses, transmission electron microscopy (TEM), histological analysis and western blotting, as described below.

Mitochondrial bioenergetics

All mitochondrial bioenergetic experiments were performed in vitro using permeabilised muscle fibres prepared from fresh muscle samples that were immediately placed in ice-cold BIOPS containing (in mmol/l): 50 MES, 7.23 K_2EGTA, 2.77 CaK_2EGTA, 20 imidazole, 0.5 dithiothreitol (DTT), 20 taurine, 5.77 ATP, 15 PCr and 6.56 $MgCl_2 \cdot 6H_2O$ (pH 7.1), as previously described in detail [13].

Mitochondrial respiration Using the Oxygraph-2k (Oroboros Instruments, Innsbruck, Austria), high-resolution measurements of mitochondrial oxygen consumption were conducted in permeabilised myofibres placed in 2 ml of respiration medium MiR05 [15], containing 0.5 mmol/l EGTA, 10 mmol/l KH_2PO_4, 3 mmol/l $MgCl_2 \cdot 6H_2O$, 60 mmol/l K-lactobionate, 20 mmol/l Hepes, 20 mmol/l taurine, 110 mmol/l sucrose and 1 mg/ml fatty acid-free BSA (pH 7.1), at 37°C. Experiments were conducted at an initial oxygen concentration of 350–375 μmol/l with constant stirring at 750 rev/min. Respiration medium was supplemented with 20 mmol/l creatine (C0780;

Table 1 Demographics of participants

Characteristic	Control ($n = 12$)	Type 1 diabetes ($n = 12$)
Sex (male/female)	5/7	5/7
Age (years)	26 ± 2	26 ± 4
Weight (kg)	65.4 ± 12.1	73.0 ± 13.4
Height (m)	1.70 ± 0.07	1.69 ± 0.13
BMI (kg/m^2)	22.5 ± 2.8	25.4 ± 3.7*
HbA_{1c} (mmol/mol)	33.0 ± 2.2	63.0 ± 16.0***
HbA_{1c} (%)	5.2 ± 0.2	7.9 ± 1.5***
Diabetes duration (years)	–	15.2 ± 7.9
Diabetes onset (years of age)	–	11.5 ± 7.3
Physical activity (min/week)[a]	233.1 ± 152.6	201.0 ± 168.6

Data are means ± SD

[a] Based on a 7 day activity recall record of moderate-to-vigorous activity levels

*$p < 0.05$, ***$p < 0.001$ vs control participants; unpaired, two-tail Student's t test

Sigma, St Louis, MO, USA) to enhance mitochondrial phosphate shuttling [16]. ADP-stimulated respiratory kinetics were determined through ADP (A5285; Sigma) titrations in the presence of 5 mmol/l blebbistatin (CAY13013; Cayman Chemical, Ann Arbor, MI, USA), in order to prevent spontaneous contraction of fibres [13, 17, 18], 5 mmol/l pyruvate (P2256; Sigma) and 2 mmol/l malate (M1000; Sigma). Complex I kinetics were determined through standard pyruvate and glutamate (GLU303; BioShop, Burlington, ON, Canada) titrations in the presence of 5 mmol/l blebbistatin, 5 mmol/l ADP and 2 mmol/l malate, while Complex II kinetics were determined through standard succinate (S2378; Sigma) titrations in the presence of 5 mmol/l blebbistatin, 5 mmol/l ADP and 10 μmol/l rotenone (R8875; Sigma; to prevent superoxide generation at Complex I). During each titration, Cytochrome *c* (192-10; Lee Biosolutions, Maryland Heights, MO, USA) was added last to determine intactness of the outer mitochondrial membrane. Any samples that exceeded a 10% increase in respiration after Cytochrome *c* addition were excluded [19].

Mitochondrial H_2O_2 emission Mitochondrial H_2O_2 emission was measured fluorometrically (QuantaMaster 40; HORIBA Scientific, Edison, NJ, USA) at 37°C in buffer Z [18], containing 105 mmol/l K-MES, 30 mmol/l KCl, 10 mmol/l KH_2PO_4, 5 mmol/l $MgCl_2 \cdot 6\ H_2O$, 1 mmol/l EGTA, 5 mg/ml BSA (pH 7.1), supplemented with 20 mmol/l creatine, 10 μmol/l Amplex UltraRed reagent (A36006; Life Technologies, Carlsbad, CA, USA), 0.5 U/ml horseradish peroxidase (P8375; Sigma) and 40 U/ml Cu/Zn superoxide dismutase (SOD1; S9697; Sigma), as described previously [13]. Various sites were assessed by titrating the following substrates [20, 21]: (1) 2.5 μmol/l antimycin (A8674; Sigma) for assessment of Complex III; (2) 10 mmol/l pyruvate and 2 mmol/l malate, to assess Complex I via generation of NADH; (3) 10 mmol/l succinate, to assess Complex I (via reverse flow) via generation of $FADH_2$; (4) 10 mmol/l pyruvate and 0.5 μmol/l rotenone, to assess pyruvate dehydrogenase complex (PDC); rotenone blocks NADH entry into Complex I; and (5) 20 mmol/l glycerol-3-phosphate, for the assessment of mitochondrial glycerol-3-phosphate dehydrogenase (mG3PDH; G7886; Sigma). In addition, fibres used for Complex I (pyruvate + malate), PDC and mG3PDH measurements were treated with 35 μmol/l 1-chloro-2,4-dinitrobenzene (237329; Sigma) during permeabilisation to deplete glutathione [22].

Mitochondrial Ca^{2+} retention capacity Mitochondrial Ca^{2+} retention capacity (CRC) was measured in duplicate, fluorometrically (QuantaMaster 40; HORIBA Scientific), at 37°C in buffer Y, containing 250 mmol/l sucrose, 10 mmol/l Tris-HCl, 20 mmol/l Tris base, 10 mmol/l KH_2PO_4, 2 mmol/l $MgCl_2 \cdot 6H_2O$ and 0.5 mg/ml BSA, with 1 μmol/l Calcium Green-5N (C3737; Life Technologies), as described previously [23]. Briefly, Ca^{2+} uptake was initiated with 8 nmol pulses of Ca^{2+} ($CaCl_2$) and then subsequent pulses of 4 nmol Ca^{2+} were titrated until opening of the mitochondrial permeability transition pore (mPTP) was observed [23].

TEM

Fresh muscle was immediately fixed in 2% (vol./vol.) glutaraldehyde (111-30-8; Electron Microscopy Sciences, Hatfield, PA, USA) in 0.1 mol/l sodium cacodylate buffer pH 7.4 (Canemco, Lakefield, QC, Canada) and processed as described previously [24]. To quantify mitochondria, representative micrographs from eight unique fibres (containing a portion of the subsarcolemmal region adjacent to the nucleus, with most of the image containing the intermyofibrillar area) were acquired at ×15,000 magnification. Blinded quantification of mitochondrial size (mean area, μm^2), distribution (number per μm^2) and density ($\mu m^2 \times$ number per $\mu m^2 \times 100$) was achieved using Nikon Imaging Software (NIS)-Elements AR (v 4.6; Nikon, Melville, NY, USA) by manually outlining mitochondria and converting to actual size using a calibration grid [25].

Electron tomography

Samples were oriented and trimmed to allow longitudinal sectioning of fibres, which were visually localised. Ultra-microtomy (Leica UC7; Leica Microsystems, Wetzlar, Germany) was performed with a 35° diamond knife (Diatome, Nidau, Switzerland), and 65 nm thick sections were mounted onto copper slot grids (Plano, Wetzlar, Germany). Electron micrographs for tomography tilt series were acquired on a JEM-2200FS electron microscope (JEOL, Akishima, Tokyo, Japan) (200 kV) equipped with a TemCam-F416 camera (TVIPS, Munich, Germany) and using a 25 electron volt (eV) energy filter slit. Under-focus was adjusted to 4000 nm. Micrographs were acquired two-fold binned for tomography. The resulting pixel size was 2.4 nm. Tilt series was collected over a total angular tilt range from −70° to +70°, at 2° increments. Image series was aligned by patch tracking mode using the IMOD software package (v 4.7; http://bio3d.colorado.edu/imod) [26]. A single reconstructed volume was computed from each tilt series by radially weighted back projection. A 3D density distribution (tomogram) was obtained. A virtual section with a 24 nm thickness was generated with the slicer tool in IMOD. Major organelles were coloured utilising Adobe Photoshop CC 2015 by a blinded researcher.

Histology and immunofluorescence analysis

Biopsied muscle was immediately embedded in Tissue Tek optimum cutting temperature (O.C.T.) compound (4583; VWR, Radnor, PA, USA), frozen in liquid nitrogen-cooled isopentane and stored at −80°C until analysis. Cryosections (−20°C) that were 8 μm thick were transferred onto static-free microscope slides (CA48311-703; VWR), allowed to air dry and fixed with ice-cold 4% (wt/vol.) paraformaldehyde. Sections were then incubated in blocking solution (5% [vol./vol.] normal goat serum in 1X PBS; S-1000; Vector Laboratories, Burlingame, CA, USA) for 30 min and then co-stained with CD31 (platelet endothelial cell adhesion molecule-1 [PECAM-1]) overnight. An antibody against CD41 was added the following day and incubated for 1 h. The appropriate secondary antibodies were then applied for 1 h: Alexa Fluor 594 and Alexa Fluor 488. Nuclei were counterstained with DAPI. CD31 was used as a marker of capillary content and CD41 to measure platelet aggregation. The antibodies were validated by manufacturers for immunofluorescence analyses (see electronic supplementary material [ESM] Table 1 for antibody details). H&E stains were used for the determination of muscle fibre area in order to calculate capillary:fibre ratio, as previously described [14]. Images were captured with a Nikon 90 Eclipse microscope (Nikon) and analysed using NIS-Elements AR software (v 4.6; Nikon) at original magnification of ×40.

Western blotting

A portion of muscle was quickly snap-frozen and stored at −80°C until analysis. Frozen muscle (~10–30 mg) was homogenised with a tapered teflon pestle in ice-cold buffer containing 40 mmol/l Hepes, 120 mmol/l NaCl, 1 mmol/l EDTA, 10 mmol/l $NAHP_2O_7{\cdot}10H_2O$ pyrophosphate, 10 mmol/l β-glycerophosphate, 10 mmol/l NaF and 0.3% CHAPS detergent (pH 7.1, adjusted using KOH). Protein concentrations were determined using a BCA assay (Life Technologies) and then loaded equally (50 or 100 μg), using Ponceau S (P7170; Sigma) as a loading control. Proteins were separated by SDS-PAGE, transferred to polyvinylidene fluoride membrane, blocked for 1 h and incubated overnight at 4°C using commercially available antibodies validated by manufacturers for western blotting: human total oxidative phosphorylation cocktail (OXPHOS; to detect individual complexes of the electron transport chain [I, II, III, IV, V]), phosphorylated (Thr172) and total AMP-activated protein kinase (AMPKα), phosphorylated (Ser555) and total Unc-51-like autophagy activating kinase 1 (ULK1), sequestosome (SQSTM1; herein referred to as p62) and vinculin. After overnight incubation, membranes were washed in tris-buffered saline, 0.1% (vol./vol.) Tween 20 (TBS-T) and incubated for 1 h at room temperature with anti-mouse infrared fluorescent secondary antibody (IRDye 800CW-conjugated) for OXPHOS, and horseradish peroxidase conjugated secondary antibody for all other proteins (see ESM Table 1 for antibody details). Immunoreactive proteins were detected by infrared imaging (Odyssey CLx; LI-COR Biosciences, Lincoln, NE, USA) or chemiluminescence (Gel Logic 6000 Pro Imager; Carestream, Rochester, NY, USA) and quantified by densitometry using Image J (v 1.51t; http://imagej.nih.gov/ij/).

Statistical analysis

All results are expressed as mean ± SEM except for participant characteristics, which are expressed as mean ± SD. An unpaired two-tailed Student's *t* test was performed for all experiments except for CRC and mitochondrial respiration kinetics where an unpaired one-tailed *t* test and a two-way ANOVA were used, respectively. Significance was established at $p \leq 0.05$.

Results

Skeletal muscle mitochondrial bioenergetics

Control of oxidative phosphorylation by ADP ADP is a primary regulator of mitochondrial bioenergetics and signals the net cellular metabolic demand to mitochondria in times of energetic stress. Therefore, we first determined if mitochondria were sensitive to low, physiologically relevant concentrations of ADP, as well as maximal concentrations (oxidative capacity) in type 1 diabetes. We found that both sensitivity to low ADP levels and maximal capacity for respiration were significantly lower ($p < 0.05$, main effect) in participants with type 1 diabetes compared with control participants (Fig. 1a).

Substrate-specific impairments We then determined if mitochondrial sensitivity to specific substrates was different in the muscle of those with type 1 diabetes vs control individuals. No detectable change in Complex I-supported mitochondrial respiration was observed, as evidenced by the lack of a significant difference in the sensitivity or capacity of the mitochondria to oxidise pyruvate (an index of glucose oxidation) (Fig. 1b). This suggests that mitochondrial oxidation of pyruvate from glucose is not impaired in type 1 diabetes, and neither is Complex I oxidation of NADH from pyruvate dehydrogenase. There were also no detectable changes in glutamate-supported respiration (NADH oxidation) (Fig. 1c), which further suggests there is no deficiency in Complex I activity in type 1 diabetes. In contrast, Complex II-supported respiration by succinate ($FADH_2$ synthesis) was significantly lower ($p < 0.001$, main effect) at both low (sensitivity) and maximal (oxidative capacity) succinate concentrations in participants with type 1 diabetes, suggesting a reduction in

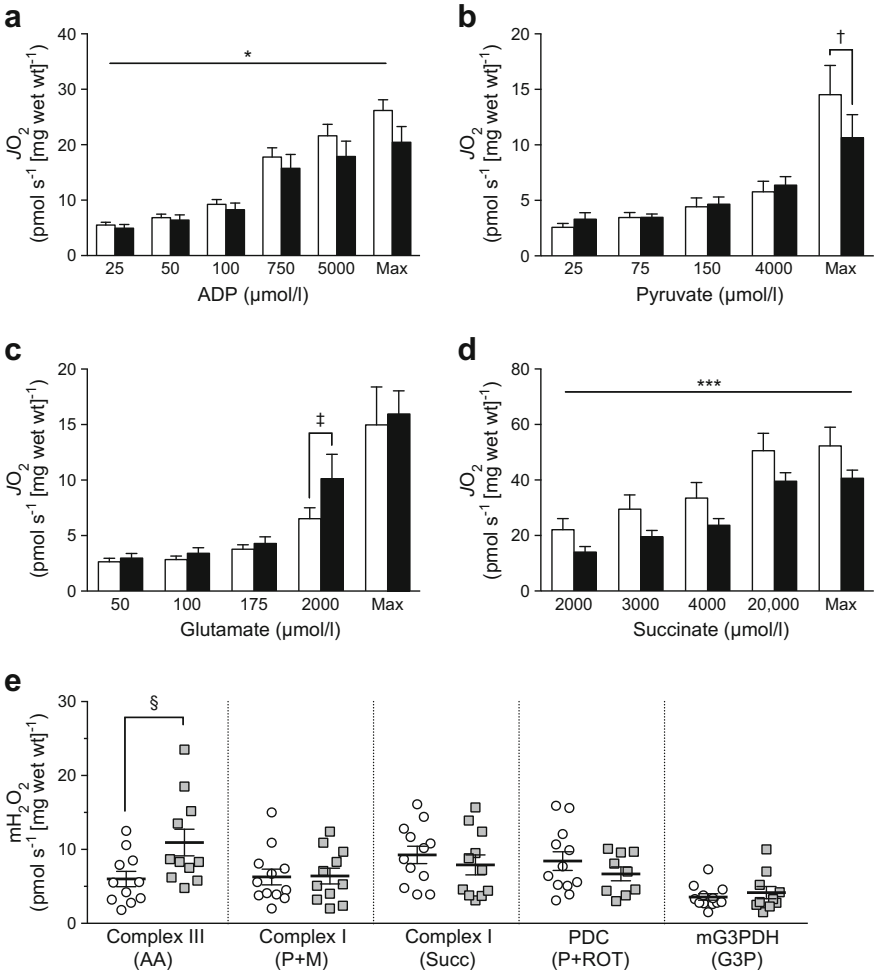

Fig. 1 Skeletal muscle mitochondrial bioenergetics in young adults with and without type 1 diabetes. Rates of mitochondrial oxygen consumption (JO_2) were measured in permeabilised muscle fibres in the presence of carbohydrate-derived substrates. (**a**) Submaximal and maximal (oxidative capacity) ADP-stimulated respiration in the presence of pyruvate and malate. Concentrations of ADP required to reach maximum varied between 6 and 18 mmol/l (both groups, $n = 12$). (**b**) Pyruvate-supported respiration (Complex I sensitivity and oxidative capacity) in the presence of 5 mmol/l ADP. Concentration of pyruvate required to reach maximum varied between 6 and 38 mmol/l (control group, $n = 11$; type 1 diabetes group, $n = 9$). (**c**) Glutamate-supported respiration (Complex I sensitivity and oxidative capacity) in the presence of 5 mmol/l ADP. Concentration of glutamate required to reach maximum varied between 4 and 20 mmol/l (control group, $n = 12$; type 1 diabetes group, $n = 8$). (**d**) Succinate-supported respiration (Complex II sensitivity and oxidative capacity) in the presence of 5 mmol/l ADP and rotenone. Concentration of succinate required to reach maximum varied between 22 and 26 mmol/l (both groups, $n = 11$). (**e**) Rates of mitochondrial H_2O_2 emission (mH_2O_2) derived from Complex III (antimycin A [AA]), Complex I forward electron flow (pyruvate + malate [P + M]) and reverse electron flow (succinate [Succ]), PDC (pyruvate + rotenone [P + ROT]) and mG3PDH (glycerol-3-phosphate [G3P]). White bars, control; black bars, type 1 diabetes; white circles, control; grey squares, type 1 diabetes. $^{*}p < 0.05$, $^{***}p < 0.001$, main effect of type 1 diabetes; $^{\dagger}p = 0.278$; $^{\ddagger}p = 0.117$; $^{\S}p < 0.05$. Max, maximum; Wt, weight

Complex II activity in type 1 diabetes compared with control individuals (Fig. 1d).

Mitochondrial H_2O_2 emission Next, we measured mitochondrial H_2O_2 emission potential. In the participants with type 1 diabetes, Complex III-supported mitochondrial H_2O_2 emission was significantly elevated ($p < 0.05$) compared with control participants but was not statistically different at Complex I (reverse [succinate] and forward electron flow [pyruvate + malate]), PDC and mG3PDH (Fig. 1e).

Skeletal muscle mitochondrial content

Considering that a reduction in mitochondrial respiration can be caused by lower mitochondrial content, we next examined the spatial organisation and abundance of mitochondria, as well as the expression of individual electron transport chain proteins. Using TEM, no differences in mean mitochondrial size, number of mitochondria per muscle area or mitochondrial area density in either the subsarcolemmal or intermyofibrillar regions of the muscle

were observed (Fig. 2a). Similarly, the levels of individual proteins were not significantly different between type 1 diabetes and control participants (Fig. 2b, c), further supporting no difference in total muscle mitochondrial content between the groups. Likewise, there were no differences in p-AMPKα^{Thr172} (relative to total AMPKα; Fig. 3d), a known regulator of mitochondrial biogenesis [27]. Collectively, this data indicates that the lower respiration per mg of muscle was not due to reductions in mitochondrial content, suggesting that impairments intrinsic to the mitochondria themselves might exist in people with type 1 diabetes. However, no differences were observed in ADP-stimulated respiration, Complex I (pyruvate)- and Complex II (succinate)-supported respiration when normalised to OXPHOS protein content (ESM Fig. 1).

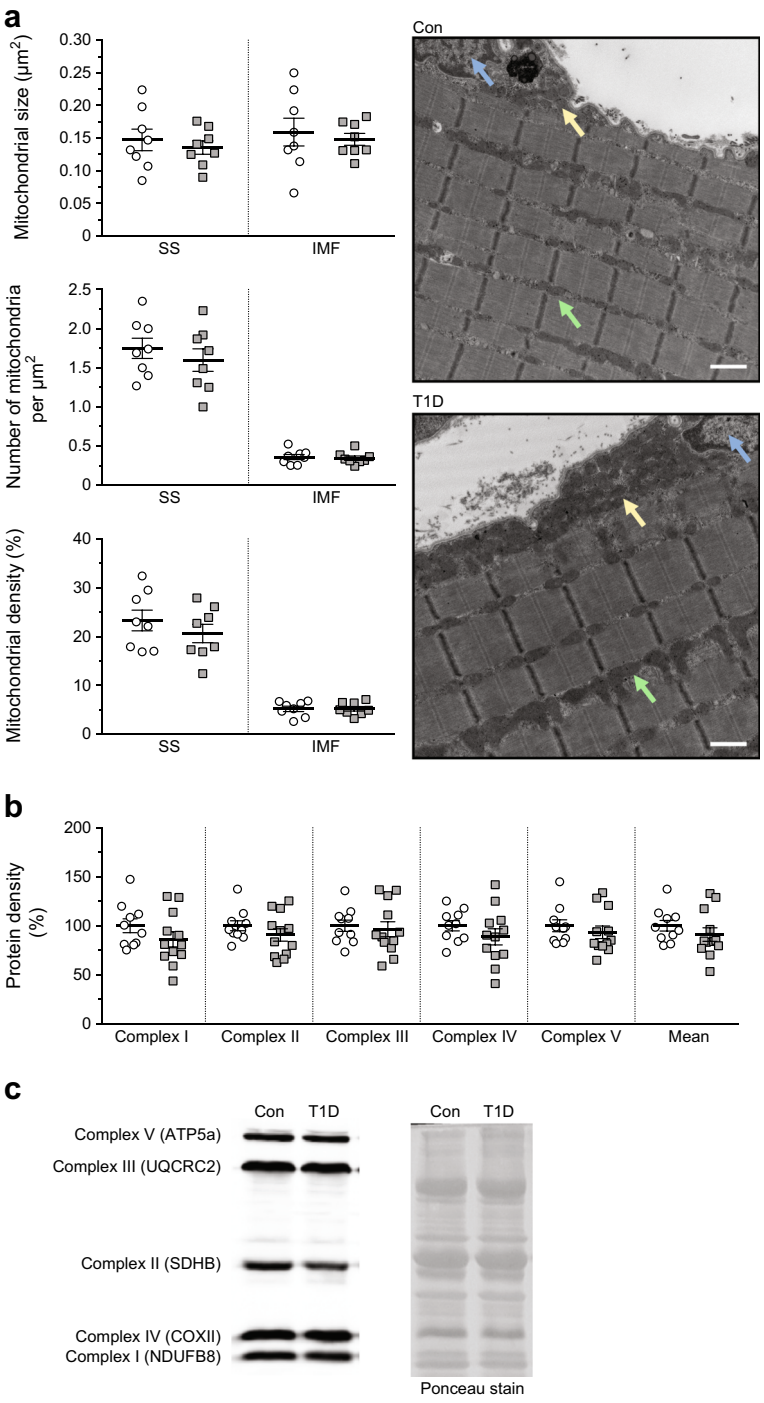

Fig. 2 Skeletal muscle mitochondrial content. (**a**) Transmission electron micrographs were acquired and analysed for mitochondrial size (mean area, μm^2), distribution (number per μm^2) and density ($\mu m^2 \times$ number per $\mu m^2 \times 100$) within the subsarcolemmal area (SS) and intermyofibrillar area (IMF) of the muscle. Blue arrow, nucleus; yellow arrow, SS mitochondria; green arrow, IMF mitochondria. Scale bar, 2 μm. (**b**) Protein levels of the individual complexes of the electron transport chain (I, II, III, IV, V; as measured by the OXPHOS antibody cocktail) as well as mean expression of all complexes combined. (**c**) Representative immunoblot of Complex I (~18 kDa), Complex II (~29 kDa), Complex III (~48 kDa), Complex IV (~22 kDa) and Complex V (~54 kDa) and Ponceau stain (loading control). White circles, control; grey squares, type 1 diabetes. ATP5a, ATP synthase subunit alpha 5; Con, control; COXII, cytochrome oxidase subunit II; NDUFB8, NADH: ubiquinone oxidoreductase subunit B8; SDHB, succinate dehydrogenase [ubiquinone] iron-sulfur subunit B; T1D, type 1 diabetes; UQCRC2, ubiquinol-cytochrome c reductase core protein 2

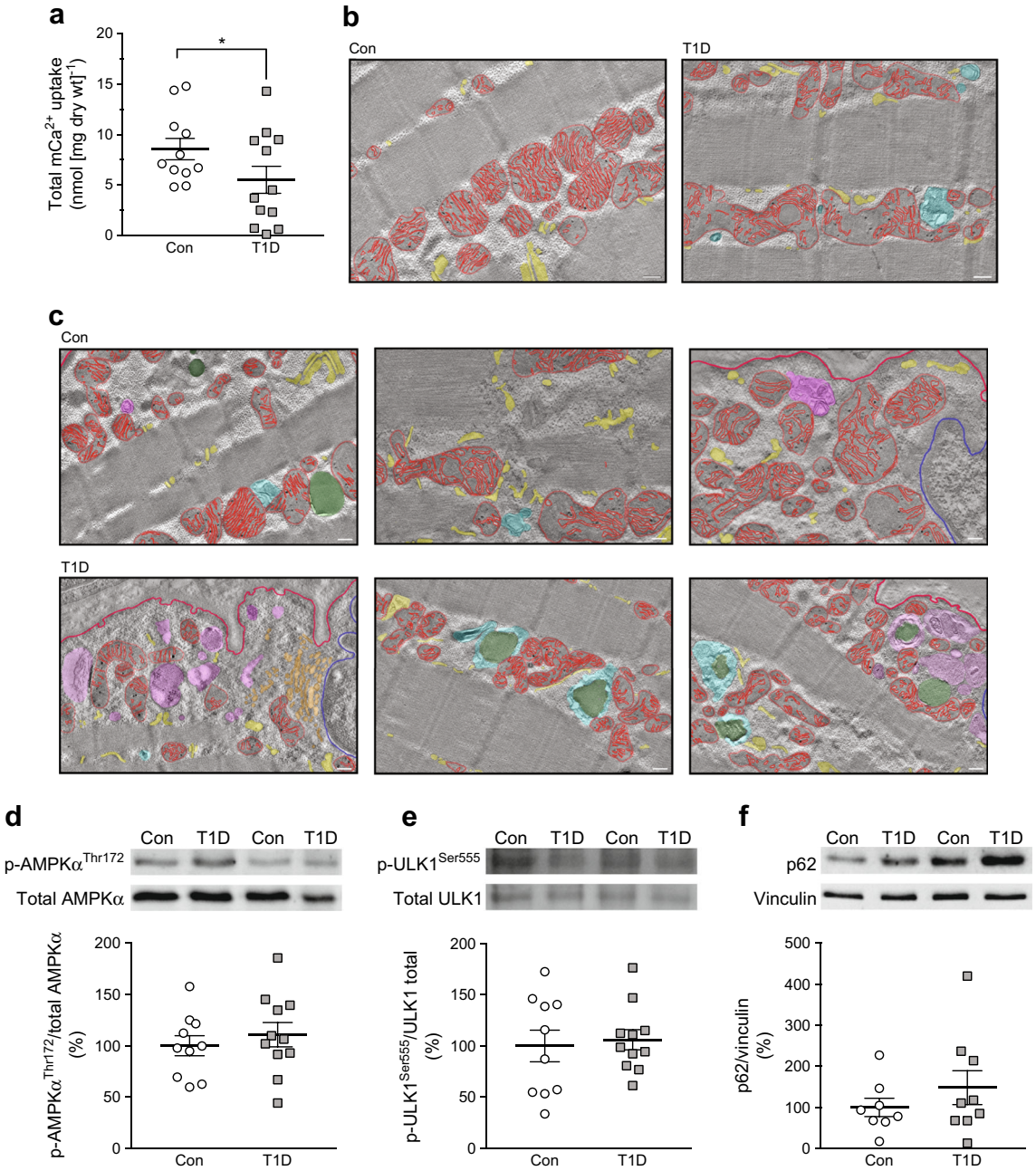

Fig. 3 Mitochondrial CRC, ultrastructural analysis and measurement of autophagic regulatory proteins. (**a**) Total mitochondrial Ca^{2+} (mCa^{2+}) uptake (a.k.a. CRC) was measured in permeabilised muscle fibres by sequential titrations of Ca^{2+} pulses until opening of the mPTP was observed. (**b**) Representative electron tomography (3D) images of irregular organisation of mitochondrial cristae (highlighted in red) in type 1 diabetes compared with control individuals. Cyan highlighting, intermyofibrillar autophagic remnants; yellow highlighting, triads/sarcoplasmic reticulum. Scale bar, 200 nm. (**c**) Representative electron tomography (3D) images of increased presence of autophagic remnants in both subsarcolemmal (highlighted in purple) and intermyofibrillar (highlighted in cyan) regions of the muscle, which were also frequently associated with intramyocellular lipid droplets (highlighted in green) in those with type 1 diabetes vs control individuals. Red highlighting, mitochondrial cristae; magenta outline, subsarcolemma; blue outline, nucleus; yellow highlighting, triads/sarcoplasmic reticulum; orange highlighting, Golgi apparatus. Scale bar, 200 nm. (**d**) Quantification of p-AMPKα^{Thr172} normalised to total AMPKα with representative blot (p-AMPKα^{Thr172} and total AMPKα, ~62 kDa). (**e**) Quantification of p-ULK1^{Ser555} normalised to total ULK1 with representative blot (p-ULK1^{Ser555} and total ULK1, ~150 kDa). (**f**) Quantification of p62 normalised to loading control vinculin, with representative blot (p62, ~62 kDa; vinculin, ~124 kDa). White circles, control; grey squares, type 1 diabetes. *$p < 0.05$. Con, control; T1D, type 1 diabetes

Instead, a main effect ($p < 0.05$) for higher Complex I (glutamate)-supported respiration was observed in those with type 1 diabetes vs control participants when normalised to OXPHOS (ESM Fig. 1c). However, we take caution in this observation given the heterogeneity in both respiration and OXPHOS protein expression

between individuals, which may warrant larger sample sizes for such ratiometric comparisons.

Skeletal muscle mitochondrial Ca^{2+} tolerance and electron tomography

We next tested Ca^{2+} handling within the mitochondria. Opening of the mPTP has been linked to swelling and energetic dysfunction [28]. We hypothesised that reductions in Ca^{2+} handling within the mitochondria (i.e. reduced CRC) would lead to an increased sensitisation of the mPTP and, ultimately, attenuations in mitochondrial respiratory function. As hypothesised, mitochondrial CRC was significantly lower ($p = 0.046$) in skeletal muscle from participants with type 1 diabetes relative to control participants (Fig. 3a).

We next used electron tomography to assess the skeletal muscle ultrastructure. This powerful technique allows for the 3D study of cellular architecture at the nanoscale level. Consistent with our observed attenuations in mitochondrial respiration, electron tomography revealed irregularities in the organisation of cristae in the participants with type 1 diabetes that were uncommon in control participants (Fig. 3b; mitochondria and cristae highlighted in red). Furthermore, consistent with the reductions in mitochondrial Ca^{2+} handling previously noted, the muscles from participants with type 1 diabetes also exhibited an increase in size and number of autophagic remnants compared with the control group, and this was visible within both the subsarcolemmal and intermyofibrillar areas (Fig. 3c; highlighted in purple and cyan, respectively). A close association of autophagic remnants to intramyocellular lipid droplets was also frequently observed in individuals with type 1 diabetes (Fig. 3c; lipid droplets highlighted in green). Despite these observations, no differences in the autophagic regulatory protein p-AMPKα^{Thr172} (as noted previously) or its downstream targets p-ULK1^{Ser555} or p62 were observed between groups (Fig. 3d–f).

Skeletal muscle microvasculature

To ascertain whether changes in mitochondrial bioenergetics were the result of microvasculature loss and concomitant hypoxia, capillary density was quantified by staining frozen muscle sections with an antibody against CD31. No significant difference between groups was observed, regardless of whether the data was collated as per cent density or ratio of total number of capillaries to myofibre area (Fig. 4a). It was also worth considering that, while capillary density may not be diminished, the capillaries present may be obstructed given the reported increases in prothrombotic factors, such as plasminogen activator inhibitor 1 (PAI-1), in type 1 diabetes [29]. We speculated that there may be greater prevalence of thrombi within the capillaries of individuals with type 1 diabetes, consequently resulting in a decreased regional blood flow. We assessed platelet aggregation by co-staining frozen muscle sections for CD31 and CD41. No significant difference between groups was demonstrated in the number of $CD41^+$ areas overlaying $CD31^+$ cells (Fig. 4b) indicating that in this physically active, young adult cohort with type 1 diabetes, impairments in skeletal muscle microvasculature did not mediate the observed alterations in mitochondrial bioenergetics and ultrastructure. Moreover, this finding also suggests that deterioration in skeletal muscle quality may precede the eventual vascular complications that arise in type 1 diabetes.

Discussion

The findings of this work highlight mitochondrial and autophagic differences within the muscles of young adults with type

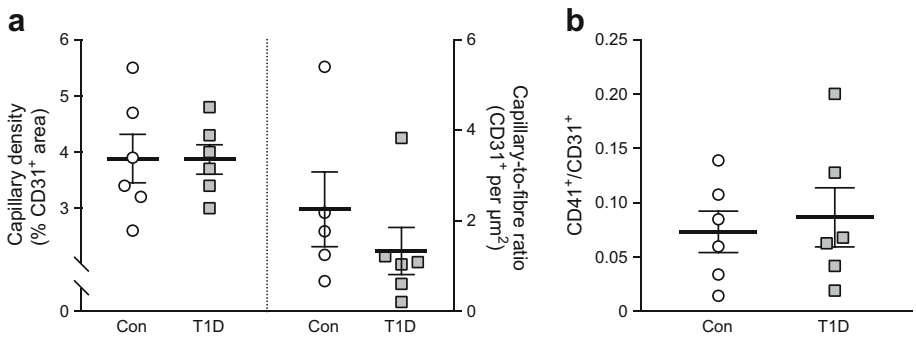

Fig. 4 Skeletal muscle capillary density and analysis of platelet aggregation. (**a**) Capillary density expressed as the percentage of areas positively stained for platelet endothelial cell adhesion molecule ($CD31^+$) relative to total muscle area analysed and as ratio of total number of $CD31^+$ to myofibre area. (**b**) Positively stained areas of platelet aggregation ($CD41^+$) within capillaries ($CD31^+$) measured as the ratio of $CD41^+$ to $CD31^+$. White circles, control; grey squares, type 1 diabetes. Con, control; T1D, type 1 diabetes

1 diabetes with moderate glycaemic control and who exceed recommended activity levels (>150 min of moderate-to-vigorous intensity activity per week) according to the American and Canadian diabetes associations [30, 31]. Specifically, the work described herein demonstrates, for the first time, site-specific alterations within the mitochondria of young adults with type 1 diabetes compared with (matched) control participants without diabetes. These alterations in mitochondrial bioenergetics occur in the absence of a loss of mitochondrial content or changes in skeletal muscle microvasculature (as assessed by capillary density and platelet aggregation). Furthermore, TEM investigations revealed that type 1 diabetes negatively affects skeletal muscle ultrastructure, as evidenced by disorganised mitochondrial cristae and an increased presence of autophagic remnants. These early alterations precede the well-characterised complications (e.g. cardiovascular disease, polyneuropathy) of type 1 diabetes and occur in large, proximal muscle groups (in contrast to distal limb muscles, which are more readily affected by polyneuropathy), suggesting that the early alterations seen in this study are unlikely to be owing to neuropathy but, instead, intrinsic alterations in muscle, and that this skeletal muscle metabolic dysregulation is a primary outcome of this chronic disease that may contribute to dysglycaemia.

Skeletal muscle is not only the primary organ system responsible for physical capacity but is also a critical metabolic organ since it is: (1) the major site of fatty acid catabolism [32]; (2) a principal mediator of whole-body glucose homeostasis [2]; and (3) a major determinant of whole-body insulin sensitivity [2, 3]. Thus, impairments in skeletal muscle quality, particularly in conditions of metabolic disease (e.g. diabetes mellitus), could have profound long-term consequences by increasing the incidence of primary contributors to the development of diabetic complications, such as recurrent dysglycaemia, dyslipidaemia and insulin resistance [33–35]. Consistent with the importance of skeletal muscle in overall health, if one considers other chronic diseases (e.g. heart disease and cancer), loss of muscle mass, strength and metabolic function (referred to as cachexia) are commonly observed, and this decline in muscle health is an important determinant in overall survival [36, 37].

While changes in skeletal muscle health of rodent models of type 1 diabetes has been more intensely studied (previously referred to as 'diabetic myopathy' [38, 39]), the extent to which this is happening in human skeletal muscle of those with type 1 diabetes has yet to be fully elucidated [40]. In the clinical diabetes literature, skeletal muscle mitochondrial ATP synthesis is one of the most widely investigated variables, often assessed indirectly in vivo by monitoring the resonance of phosphate in ATP using ^{31}P-MRS. Previous studies using ^{31}P-MRS have frequently, but not always [41], reported a ~20–25% reduction in mitochondrial ATP synthesis rates in the skeletal muscle of those with type 1 diabetes [9–11]. While ^{31}P-MRS has the obvious advantage of capturing ATP kinetics under intact physiological conditions, a drawback of this approach is the lack of mechanistic understanding underlying the changes in mitochondrial function that may be observed.

Consistent with the work of Cree-Green et al [9] and others [10, 11], we observed a ~20% reduction in mitochondrial oxidative capacity in the muscles of those with type 1 diabetes (Fig. 1a, Max), suggesting that our in vitro (permeabilised muscle fibre method) assessment is consistent with ^{31}P-MRS studies. What was unanswered from the aforementioned ^{31}P-MRS studies, however, was whether the mitochondria are reduced in content and/or impaired, or whether nutrient delivery is the cause of the resulting poor mitochondrial function in those with type 1 diabetes. Here we provide the mechanistic insight to answer these questions.

First, regarding whether the deficits observed in previous ^{31}P-MRS studies were directly related to differences in mitochondrial content or impairments of mitochondrial quality, we now offer invaluable insight using ultrastructural analysis. Using TEM, we observed no difference in the amount, distribution and size of mitochondria within the skeletal muscle of those with type 1 diabetes compared with control individuals. Within the mitochondria, we observed no differences in the protein expression of the individual electron transport chain protein subunits using western blot analysis (total OXPHOS cocktail), further suggesting that mitochondrial content is not reduced in young, physically active adults with type 1 diabetes vs control individuals. In contrast, we did observe structural abnormalities in mitochondria using electron tomography; disorganised cristae and more abundant autophagic structures were present in the muscles of individuals with type 1 diabetes compared with control participants. In line with this, we also observed a significant reduction in mitochondria viability in permeabilised myofibres of those with type 1 diabetes, as assessed by CRC [23].

Second, these findings suggest that nutrient delivery in the muscles of young adults with type 1 diabetes is not likely impaired. Histological/immunofluorescent examination of skeletal muscle biopsies revealed that capillary density within the vastus lateralis muscle was not different between those with type 1 diabetes and those without. Furthermore, as increases in prothrombotic factors have been reported in those with type 1 diabetes [29], we investigated whether the capillaries present were occluded by platelet aggregates (thrombi) and found that they were not. While we do not see visible evidence for impaired blood flow in the present study, we cannot rule out the possibility of a functional impairment resulting in reduced blood flow and delivery of oxygen and nutrients within the muscles of those with type 1 diabetes [42].

Collectively, these novel results provide evidence of direct alterations in skeletal muscle mitochondria in those with type 1 diabetes. The underlying mechanism(s) for these mitochondrial alterations in type 1 diabetes may be revealed by the

mitochondrial bioenergetics investigations related to mitochondrial H_2O_2 emission in this study. To the best of our knowledge, mitochondrial-derived ROS production has never been examined in skeletal muscle of humans with type 1 diabetes. We observed a significant increase in mitochondrial H_2O_2 emission potential at the level of Complex III, with no significant differences owing to Complex I, intermembrane (mG3PDH) or matrix (PDC) proteins. Work using isolated mitochondria [43, 44], has demonstrated that Complex III significantly contributes to ROS production in response to fatty acid oxidation. While we did not assess this in the current study, future work should be undertaken to discern differences in the propensity for ROS production at Complex III in response to glucose and lipid substrate availability in those with type 1 diabetes. The tissue requirements for the comprehensive assessment of mitochondrial phenotype prohibited additional assessment of major mitochondrial antioxidant enzymes (e.g. glutathione peroxidase, thioredoxin reductase and superoxide dismutase) and markers of oxidative stress in the present study. Nonetheless, it has been suggested that Complex III-generated ROS serves as a signalling molecule, particularly in the adaptive response to hypoxia (for review see [45]). This latter point may be physiologically important when considering the peripheral vascular disease that is known to develop in older adults with type 1 diabetes.

Perspectives

This investigation revealed that young, active people with type 1 diabetes possess mitochondrial and muscle ultrastructural abnormalities that precede reductions in capillary content. While we have demonstrated site-specific alterations in mitochondrial bioenergetics, further investigation is required to identify the precise signalling pathway leading to these changes. Though our observations of increased autophagic remnants in muscles of those with type 1 diabetes were not associated with increases in autophagic markers (p-ULK1^{Ser555} and p62), it is possible that these signals had already been transmitted and pathways initiated. Alternatively, recent work [46] has suggested that p62 activity is redox sensitive and may promote autophagy in the absence of changes in content. Clearly, future work in this area will help further elucidate this important observation.

It seems likely that the relationship between skeletal muscle abnormalities and dysglycaemia in type 1 diabetes are reciprocal, particularly given previous suggestions that excessive glucose provision to mitochondria elevates ROS production [47, 48]. Another possible mechanism may relate to peripheral insulin administration. Specifically, in people without type 1 diabetes, large rises in blood glucose levels following a glucose load are attenuated by delivering insulin to the liver first via the portal circulation. However, in those with type 1 diabetes, peripheral insulin administration bypasses the canonical 'liver-first' model and results in greater elevations in circulating blood glucose [49]. The peripheral insulin administration shifts a greater burden of the glycaemic load to skeletal muscle, forcing it to accept a greater glycaemic load then it otherwise would [1, 2], thereby increasing glycaemic stress akin to that previously described [50] for cell types that could not regulate cellular glucose entry. An important avenue for future research is to investigate this altered relationship between blood glucose levels, peripheral insulin injections and the muscle abnormalities reported in the type 1 diabetes population. Indeed, this relationship might be considered in the context of potential cellular abnormalities in other relevant tissues, such as liver and adipose tissue.

A major clinical concern in this study is that the mitochondrial/metabolic alterations observed were in young adults with type 1 diabetes, who had self-reported moderate-to-vigorous activity levels above the American and Canadian diabetes associations' recommendations. In addition, these changes occurred in large, proximal muscle groups without a detectable loss of capillary density. Clearly, larger cohort studies are needed to assess the impact of type 1 diabetes in those who are sedentary, as well as those who meet or exceed physical activity recommendations, to determine whether an optimal level of physical activity exists that is sufficient to restore/overcome the metabolic abnormalities that characterise the muscle of those with type 1 diabetes.

Acknowledgements The authors are extremely grateful and thankful to all the participants for their contributions (time and tissue) to this study. The authors also thank A. N. Belcastro (School of Kinesiology and Health Science, York University, Toronto, ON, Canada) for access to his human clinical laboratory. The authors express their appreciation to J. Hanson (Executive Director; Connected in Motion, ON, Canada) for her assistance with participant recruitment, K. Mackett (McMaster University, Hamilton, ON, Canada) for her assistance in data analysis and G. R. Steinberg (Department of Medicine, McMaster University, Hamilton, ON, Canada) for generously providing some of the antibodies used in this study.

Data availability All relevant data are included in the article.

Funding This project was funded by the Natural Sciences and Engineering Research Council of Canada (NSERC; grant 298738-2013 to TJH and grant 436138-2013 to CGRP) and the James H. Cummings Foundation (to CGRP). CMFM and MCH were recipients of NSERC graduate scholarships. CMFM was also a recipient of the DeGroote Doctoral Scholarship of Excellence. SVR was a recipient of the Ontario Graduate Scholarship. TJH and CGRP received a Canada Foundation for Innovation grant (no. 23552 and 32449, respectively).

Duality of interest The authors declare that there is no duality of interest associated with this manuscript.

Contribution statement CMFM, MCH, MAT, TJH and CGRP designed the experiments. CMFM, TJH and CGRP wrote the manuscript. CMFM, MCH, SVR, NEV, CL and CM performed experiments. CMFM, MCH, SVR, NEV, CL, FAR, CM, MAT, MPK, RL, TJH and CGRP analysed and interpreted data. All authors edited the manuscript. All authors provided final approval of the version to be published. All people

designated as authors qualify for authorship, and all those who qualify for authorship are listed. TJH and CGRP are the guarantors of this work and, as such, had full access to all the data in the study and take responsibility for the integrity of data and the accuracy of the data analysis.

References

1. DeFronzo RA, Hendler R, Simonson D (1982) Insulin resistance is a prominent feature of insulin-dependent diabetes. Diabetes 31: 795–801
2. Shulman GI, Rothman DL, Jue T et al (1990) Quantitation of muscle glycogen synthesis in normal subjects and subjects with non-insulin-dependent diabetes by 13Cnuclear magnetic resonance spectroscopy. N Engl J Med 322:223–228
3. Jensen J, Aslesen R, Ivy JL, Brørs O (1997) Role of glycogen concentration and epinephrine on glucose uptake in rat epitrochlearis muscle. Am J Phys 272:E649–E655
4. Højlund K, Beck-Nielsen H (2006) Impaired glycogen synthase activity and mitochondrial dysfunction in skeletal muscle: markers or mediators of insulin resistance in type 2 diabetes? Curr Diabetes Rev 2:375–395
5. The Diabetes Control and Complications Trial Research Group (1993) The effect of intensive treatment of diabetes on the development and progression of long-term complications in insulin-dependent diabetes mellitus. N Engl J Med 329:977–986
6. Diabetes Control and Complications Trial/Epidemiology of Diabetes Interventions and Complications Research Group, Lachin JM, Genuth S, Cleary P, David MD, Nathan DM (2000) Retinopathy and nephropathy in patients with type 1 diabetes four years after a trial of intensive therapy. N Engl J Med 342:381–389
7. Wong E, Backholer K, Gearon E et al (2013) Diabetes and risk of physical disability in adults: a systematic review and meta-analysis. Lancet Diabetes Endocrinol 1:106–114
8. Muoio DM, Neufer PD (2012) Lipid-induced mitochondrial stress and insulin action in muscle. Cell Metab 15:595–605
9. Cree-Green M, Newcomer BR, Brown MS et al (2015) Delayed skeletal muscle mitochondrial ADP recovery in youth with type 1 diabetes relates to muscle insulin resistance. Diabetes 64:383–392
10. Kacerovsky M, Brehm A, Chmelik M et al (2011) Impaired insulin stimulation of muscular ATP production in patients with type 1 diabetes. J Intern Med 269:189–199
11. Crowther GJ, Milstein JM, Jubrias SA et al (2003) Altered energetic properties in skeletal muscle of men with well-controlled insulin-dependent (type 1) diabetes. Am J Physiol Endocrinol Metab 284: E655–E662
12. Reske-Nielsen E, Harmsen A, Vorre P (1977) Ultrastructure of muscle biopsies in recent, short-term and long-term juvenile diabetes. Acta Neurol Scand 55:345–362
13. Hughes MC, Ramos SV, Turnbull PC et al (2015) Mitochondrial bioenergetics and fiber type assessments in microbiopsy vs. bergstrom percutaneous sampling of human skeletal muscle. Front Physiol 6:360
14. D'Souza DM, Zhou S, Rebalka IA et al (2016) Decreased satellite cell number and function in humans and mice with type 1 diabetes is the result of altered notch signaling. Diabetes 65:3053–3061
15. Gnaiger E, Kuznetsov AV, Schneeberger S et al (2000) Mitochondria in the cold. In: Heldmaier G, Klingenspor M (eds) Life in the cold. Springer, Berlin, pp 431–442
16. Aliev M, Guzun R, Karu-Varikmaa M et al (2011) Molecular system bioenergics of the heart: experimental studies of metabolic compartmentation and energy fluxes versus computer modeling. Int J Mol Sci 12:9296–9331
17. Perry CGR, Kane DA, Lin C-T et al (2011) Inhibiting myosin-ATPase reveals a dynamic range of mitochondrial respiratory control in skeletal muscle. Biochem J 437:215–222
18. Perry CGR, Kane DA, Lanza IR, Neufer PD (2013) Methods for assessing mitochondrial function in diabetes. Diabetes 62:1041–1053
19. Kuznetsov AV, Schneeberger S, Seiler R et al (2004) Mitochondrial defects and heterogeneous cytochrome c release after cardiac cold ischemia and reperfusion. Am J Physiol Heart Circ Physiol 286: H1633–H1641
20. Fisher-Wellman KH, Lin C-T, Ryan TE et al (2015) Pyruvate dehydrogenase complex and nicotinamide nucleotide transhydrogenase constitute an energy-consuming redox circuit. Biochem J 467:271–280
21. Wong H-S, Dighe PA, Mezera V et al (2017) Production of superoxide and hydrogen peroxide from specific mitochondrial sites under different bioenergetic conditions. J Biol Chem 292:16804–16809
22. Fisher-Wellman KH, Gilliam LAA, Lin C-T et al (2013) Mitochondrial glutathione depletion reveals a novel role for the pyruvate dehydrogenase complex as a key H2O2 emitting source under conditions of nutrient overload. Free Radic Biol Med 65: 1201–1208
23. Anderson EJ, Rodriguez E, Anderson CA et al (2011) Increased propensity for cell death in diabetic human heart is mediated by mitochondrial-dependent pathways. Am J Physiol Heart Circ Physiol 300:H118–H124
24. Nilsson MI, MacNeil LG, Kitaoka Y et al (2015) Combined aerobic exercise and enzyme replacement therapy rejuvenates the mitochondrial–lysosomal axis and alleviates autophagic blockage in Pompe disease. Free Radic Biol Med 87:98–112
25. Tarnopolsky MA, Rennie CD, Robertshaw HA et al (2007) Influence of endurance exercise training and sex on intramyocellular lipid and mitochondrial ultrastructure, substrate use, and mitochondrial enzyme activity. Am J Phys Regul Integr Comp Phys 292:R1271–R1278
26. Kremer JR, Mastronarde DN, McIntosh JR (1996) Computer visualization of three-dimensional image data using IMOD. J Struct Biol 116:71–76
27. O'Neill HM, Holloway GP, Steinberg GR (2013) AMPK regulation of fatty acid metabolism and mitochondrial biogenesis: implications for obesity. Mol Cell Endocrinol 366:135–151
28. Baines CP, Kaiser RA, Purcell NH et al (2005) Loss of cyclophilin D reveals a critical role for mitochondrial permeability transition in cell death. Nature 434:658–662
29. Joy NG, Hedrington MS, Briscoe VJ et al (2010) Effects of acute hypoglycemia on inflammatory and pro-atherothrombotic biomarkers in individuals with type 1 diabetes and healthy individuals. Diabetes Care 33:1529–1535
30. Colberg SR, Sigal RJ, Yardley JE et al (2016) Physical activity/exercise and diabetes: a position statement of the American Diabetes Association. Diabetes Care 39:2065–2079
31. Sigal RJ, Armstrong MJ, Colby P et al (2013) Physical activity and diabetes. Can J Diabetes 37:S40–S44
32. Hargreaves M (2000) Skeletal muscle metabolism during exercise in humans. Clin Exp Pharmacol Physiol 27:225–228
33. Dunn FL (1992) Plasma lipid and lipoprotein disorders in IDDM. Diabetes 41:102–106
34. Kilpatrick ES, Rigby AS, Atkin SL (2007) Insulin resistance, the metabolic syndrome, and complication risk in type 1 diabetes: "double diabetes" in the Diabetes Control and Complications Trial. Diabetes Care 30:707–712
35. Soedamah-Muthu SS, Fuller JH, Mulnier HE et al (2006) All-cause mortality rates in patients with type 1 diabetes mellitus compared with a non-diabetic population from the UK general practice research database, 1992-1999. Diabetologia 49:660–666

36. Kadar L, Albertsson M, Areberg J et al (2000) The prognostic value of body protein in patients with lung cancer. Ann N Y Acad Sci 904: 584–591
37. Anker SD, Steinborn W, Strassburg S (2004) Cardiac cachexia. Ann Med 36:518–529
38. Coleman SK, Rebalka IA, D'souza DM, Hawke TJ (2015) Skeletal muscle as a therapeutic target for delaying type 1 diabetic complications. World J Diabetes 6:1323–1336
39. D'Souza DM, Al-Sajee D, Hawke TJ (2013) Diabetic myopathy: impact of diabetes mellitus on skeletal muscle progenitor cells. Front Physiol 4:379
40. Monaco CMF, Perry CGR, Hawke TJ (2017) Diabetic myopathy: current molecular understanding of this novel neuromuscular disorder. Curr Opin Neurol 30:545–552
41. Item F, Heinzer-Schweizer S, Wyss M et al (2011) Mitochondrial capacity is affected by glycemic status in young untrained women with type 1 diabetes but is not impaired relative to healthy untrained women. Am J Phys Regul Integr Comp Phys 301:R60–R66
42. Khan F, Cohen RA, Ruderman NB et al (1996) Vasodilator responses in the forearm skin of patients with insulin-dependent diabetes mellitus. Vasc Med Lond Engl 1:187–193
43. Seifert EL, Estey C, Xuan JY, Harper M-E (2010) Electron transport chain-dependent and -independent mechanisms of mitochondrial H2O2 emission during long-chain fatty acid oxidation. J Biol Chem 285:5748–5758
44. St-Pierre J, Buckingham JA, Roebuck SJ, Brand MD (2002) Topology of superoxide production from different sites in the mitochondrial electron transport chain. J Biol Chem 277:44784–44790
45. Bleier L, Dröse S (2013) Superoxide generation by complex III: from mechanistic rationales to functional consequences. Biochim Biophys Acta BBA - Bioenerg 1827:1320–1331
46. Carroll B, Otten EG, Manni D et al (2018) Oxidation of SQSTM1/p62 mediates the link between redox state and protein homeostasis. Nat Commun 9:256
47. Leloup C, Tourrel-Cuzin C, Magnan C et al (2009) Mitochondrial reactive oxygen species are obligatory signals for glucose-induced insulin secretion. Diabetes 58:673–681
48. Munusamy S, MacMillan-Crow LA (2009) Mitochondrial superoxide plays a crucial role in the development of mitochondrial dysfunction during high glucose exposure in rat renal proximal tubular cells. Free Radic Biol Med 46:1149–1157
49. Gregory JM, Kraft G, Scott MF et al (2015) Insulin delivery into the peripheral circulation: a key contributor to hypoglycemia in type 1 diabetes. Diabetes 64:3439–3451
50. Brownlee M (2005) The pathobiology of diabetic complications. Diabetes 54:1615–1625